



Open Access

ORIGINAL ARTICLE

Sperm Biology

Stimulated by retinoic acid gene 8 (Stra8) plays important roles in many stages of spermatogenesis

Hai-Tao Ma^{1,2,*}, Chang-Min Niu^{1,2,*}, Jing Xia^{1,2}, Xue-Yi Shen^{1,2}, Meng-Meng Xia^{1,2}, Yan-Qiu Hu³, Ying Zheng^{1,2}

To clarify the functions and mechanism of stimulated by retinoic acid gene 8 (Stra8) in spermatogenesis, we analyzed the testes from *Stra8* knockout and wild-type mice during the first wave of spermatogenesis. Comparisons showed no significant differences in morphology and number of germ cells at 11 days postpartum, while 21 differentially expressed genes (DEGs) associated with spermatogenesis were identified. We speculate that *Stra8* performs many functions in different phases of spermatogenesis, such as establishment of spermatogonial stem cells, spermatogonial proliferation and self-renewal, spermatogonial differentiation and meiosis, through direct or indirect regulation of these DEGs. We therefore established a preliminary regulatory network of *Stra8* during spermatogenesis. These results will provide a theoretical basis for further research on the mechanism underlying the role of *Stra8* in spermatogenesis.

Asian Journal of Andrology (2018) 20, 479–487; doi: 10.4103/aja.aja_26_18; published online: 29 May 2018

Keywords: differentiation; meiosis; proliferation; spermatogenesis; spermatogonia; *Stra8*

INTRODUCTION

In mammals, spermatogenesis is a highly ordered and precisely regulated process, ensuring that millions of spermatozoa are produced at a constant rate. Mature sperm production depends on the stable self-renewal, proliferation, and differentiation of spermatogonial stem cells (SSCs). The A₁ spermatogonia divide successively into A₂, A₃, A₄, intermediate (In), and B spermatogonia. After a round of DNA replication, B spermatogonia undergo two rounds of meiosis to form spermatocytes, which then undergo morphological changes to become haploid sperm cells. Successful spermatogenesis occurs through precise regulation of gene expression. Stimulated by retinoic acid gene 8 (*Stra8*) is a key molecule involved in meiosis initiation and plays an important role in spermatogenesis.¹

Retinoic acid (RA), which is an active metabolite of Vitamin A, is a vital signaling molecule involved in germ cell development and correct entry into meiosis. *Stra8* was identified as RA-responsive gene by Oulad-Abdelghani in 1995.^{2,3} RA directly regulates the expression of *Stra8* via its specific nuclear hormone receptors (retinoic acid receptors [RARs] and retinoid X receptors [RXRs]). RARs form heterodimers with RXRs, which bind to the retinoic acid responsive elements (RAREs) located in the *Stra8* promoter. RA-bound RAR-RXR heterodimers activate or repress RA-responsive gene expression by recruiting histone acetyltransferase or deacetylase.^{4,5} The lack of *Stra8* expression in the embryonic testis is mainly due to the degradation of RA by cytochrome P450 26B1 (CYP26B1). However, after embryonic day 13.5 (E13.5), the expression levels of CYP26B1 gradually decrease.⁶ At this point, Nanos2 production is initiated, which mediates direct downregulation of *Stra8* expression, preventing the induction of meiosis in the germ cells in

embryonic testes and inhibiting apoptosis.⁴ Moreover, Creb-binding protein (CBP), a coactivator of histone acetyltransferase, mediates *Stra8* transcription, while p300 represses *Stra8* transcription by SUMO-1 modification.⁷ In addition, Sohlh1 and Sohlh2 repress *Stra8* expression by binding to the E-Boxes located in the promoter.⁸ DMRT1 regulates meiosis by enhancing Sohlh1 expression and repressing *Stra8* expression.⁹ To date, most studies have focused on the proteins that directly or indirectly regulate *Stra8*; however, the identities of proteins regulated by *Stra8* as well as regulatory proteins downstream of *Stra8* remain to be established. Furthermore, the functional mechanism and regulatory network of *Stra8* during spermatogenesis remain to be clarified.

In this study, we performed a histological analysis of *Stra8* knockout (*Stra8*^{-/-} KO) testes and wild-type (WT) testes during the first wave of spermatogenesis. Although there were no obvious differences in morphology or the number of germ cells at 11 days postpartum (dpp), significant differences were detected at 12 dpp. Compared with WT testes, RNA sequencing (RNA-Seq) analysis revealed 96 differentially expressed genes (DEGs) in *Stra8*^{-/-} testes, 21 of which are reported to be directly or indirectly involved in spermatogenesis. We propose a regulatory network for *Stra8* as a multifunctional protein involved in the establishment and maintenance of SSCs, cell proliferation, self-renewal, differentiation, and maintenance of the undifferentiated state during spermatogenesis.

MATERIALS AND METHODS

Mice

Heterozygous B6.Cg-*Stra8*^{tm1Dcp/J} mice (*Stra8*^{+/-} mice) were purchased from Jackson Laboratory (Bar Harbor, ME, USA) on

¹Department of Histology and Embryology, School of Medicine, Yangzhou University, Yangzhou 225001, China; ²Jiangsu Key Laboratory of Experimental and Translational Noncoding RNA Research, Yangzhou 225001, China; ³Clinical Medical College, Yangzhou University, Yangzhou 225001, China.

*These authors contributed equally to this work.

Correspondence: Dr. Y. Zheng (yzzk@163.com)

Received: 31 October 2017; Accepted: 27 February 2018

a C57BL/6 genetic background. All mice were maintained at the Laboratory Animal Center of Yangzhou University (Yangzhou, China) under conditions of controlled temperature (21°C–25°C), a 12 h/12 h light/dark cycle, and a normal diet. The day of birth was defined as 0 dpp. All animal experiments conducted as part of this study were approved by the Animal Ethics Committee of Yangzhou University.

DNA extraction and genotyping

Female and male heterozygous mice were housed together, and the genotypes of the offspring were identified following protocols provided by the Jackson Laboratory. All mice genotypes were identified by polymerase chain reaction (PCR) amplification of the DNA extracted from tail tissue. The tissue was incubated with 700 μ l Lysis buffer I and 30 μ l proteinase K (Sigma Chemical Co., St. Louis, MO, USA) for 2 h at 55°C before the DNA was obtained by phenol/chloroform extraction and ethanol precipitation.

Tail DNA was genotyped by PCR amplification using the following primers: *Stra8*-P1 (5'-CAACCAACCCAGTGATGATG-3'), *Stra8*-P2 (5'-TCAGGTCAGGCTGCTAGGAT-3'), and *Stra8*-P3 (5'-GATAGCTTGGCTGCAGGTC-3'). PCR conditions were as follows: 10 cycles of 94°C for 20 s, 65°C for 15 s, and 68°C for 10 s and 28 cycles of 94°C for 15 s, 60°C for 15 s, and 72°C for 10 s, respectively. Genotypes were identified from the PCR products separated by 1.2% (*w/v*) agarose gel electrophoresis (WT: 316 bp; mutant type [MT]: 200 bp).

Histological sample preparation and staining

Mouse testes were fixed with Bouin's solution for 4 h or 4% (*w/v*) paraformaldehyde for 24 h, then in chloroform overnight followed by dehydration in a gradient alcohol series. After transfer into xylene, testicular tissue was soaked in liquid paraffin for 2 h and then embedded in paraffin for further analysis.

Testes from 5–12 dpp and adult mice were collected, and sections were prepared (thickness, 4 μ m) for HE staining. Types of germ cells were identified by their location, nuclear size, and chromatin characteristics.

Immunofluorescence, immunohistochemistry analysis, and cell counting

Mouse testes (5–12 dpp) were fixed in 4% (*w/v*) paraformaldehyde overnight for immunofluorescence analysis. Testes from *Stra8*^{-/-} and WT mice (11 dpp) were used for immunohistochemistry. Tissues were dewaxed, treated by methanol and hydrogen peroxide, and heated in antigen repair solution (citric acid and trisodium citrate acid). After cooling, sections were blocked by incubation in donkey serum (Solarbio® Life Sciences, Beijing, China) at room temperature before incubation with primary antibodies (Ddx4, Nanos3, Egr4, Abcam, Cambridge, England; Asb9, Santa Cruz Biotechnology, Santa Cruz, CA, USA; Msh5, Biorbyt, Cambridge, England; Utf1, HuaAn Biotechnology Co., Ltd., Hangzhou, China) overnight at 4°C. On the 2nd day, sections were stained with fluorescein isothiocyanate (FITC)-labeled anti-rabbit/mouse IgG (Sigma Chemical Co.) at 37°C for 1 h and then restained with diamidino-phenyl-indole (DAPI, Solarbio® Life Sciences) for immunofluorescence analysis. Immunohistochemistry was then performed followed the protocol provided for the GT Vision™ III Detection System (Gene Tech, Shanghai, China). Images were obtained from a fluorescence microscope (Eclipse 70i, Nikon, Tokyo, Japan) and the number of Ddx4-positive cells was counted. Statistical difference between two groups was assessed by *t*-test ($n \geq 6$).

RNA sequencing

WT and homozygous testes from 11 dpp mice were collected and stored in liquid nitrogen after addition of Trizol (Life Technologies, Frederick, MD, USA). Three groups of four testes from two mice were used for RNA sequencing. Total RNA was prepared according to normal protocols. The eukaryotic mRNA was purified from total RNA using Oligo(dT) magnetic beads. After purification and terminal repair, the mRNAs were then fragmented, and double-stranded cDNA was generated for use as a template in PCR amplification to generate the complete library. The library was then analyzed in an Agilent 2100 Bioanalyzer (Agilent Technologies Co., Ltd., Palo Alto, CA, USA) and ABI StepOnePlus™ Real-Time PCR System (Applied Biosystems, Foster City, CA, USA) for quality and yield.

RNA-Seq analysis was performed by BGI Genomics Co., Ltd., Shenzhen, China. Gene expression levels were quantified using the RSEM software package, University of Tokyo, Tokyo, Japan. FPKM represents a unit of gene expression that can be used for direct comparison of the different gene expression levels of different samples. The NOISeq method was used to screen for DEGs in WT and *Stra8*^{-/-} testes. Gene ontology (GO) annotation analysis of the distribution of gene functions was performed using WEGO software (Web Gene Ontology Annotation Plot, <http://wego.genomics.org.cn/>). Pathway enrichment analysis of the interaction between genes was performed by searching the Kyoto Encyclopedia of Genes and Genomes (KEGG) database.

RNA extraction and qRT-PCR analysis

Total RNA was extracted from WT and homozygous mice testes (11 dpp) using the one-step guanidine isothiocyanate-phenol-chloroform method. After removal of genomic DNA, reverse transcription was performed according to the manufacturer's instructions. Quantitative reverse transcription-PCR (qRT-PCR) analysis was then performed using GoTaq® qPCR Master Mix (TaKaRa, Tokyo, Japan) with the primers listed in **Table 1**. The thermal cycling conditions were as follows: 40 cycles of denaturation at 95°C for 15 s, annealing at 60°C for 30 s, and elongation at 72°C for 30 s. qRT-PCR results were normalized against *Gapdh* as a reference to determine the relative expression levels of the genes.

Western blot analysis

Testis proteins from 11 dpp mice were extracted using RIPA buffer (Solarbio® Life Sciences). After centrifugation at 10 000 *g* for 15 min at 4°C, the supernatant was collected. Total proteins (50 μ g) were separated by sodium dodecyl sulfate (SDS)-polyacrylamide gel electrophoresis and transferred to a polyvinylidene difluoride membrane. After blocking in Tris-buffered saline (TBS) containing 5% (*w/v*) nonfat milk, the membrane was incubated with the primary detection antibodies (*Stra8*, Nanos3, Egr4, Pou5f1, *Gapdh*, Abcam; RhoX10, donated by Miles F Wilkinson Lab, University of California, Berkeley, CA, USA; Asb9, Dmc1, Santa Cruz; Msh5, Biorbyt) overnight at 4°C. The membranes were then incubated with secondary antibodies (ZSbio, Beijing, China) at room temperature for 1.5 h. Proteins were detected by electrogenerated chemiluminescence (ECL).

Statistical analysis

Statistical analysis was performed using SPSS18.0 (SPSS Inc., Chicago, IL, USA). Data were presented as mean \pm standard deviation (s.d.) and analyzed by Student's *t*-test. All experiments were repeated at least three times. $P \leq 0.05$ was considered to indicate statistical significance.

Table 1: Primer sequences for reverse transcription polymerase chain reaction

Name	Forward primer	Reverse primer
<i>Stra8</i>	5'-ACCCTGGTAGGGCTCTTCAA-3'	5'-GACCTCCTAAGCTGTTGGG-3'
<i>Mtl5</i>	5'-CGGGATGAGTTGCCGGTTC-3'	5'-CGGGAAGTAACGACGATAACAC-3'
<i>Egr4</i>	5'-TATCCTGGAGCGACTTCTTG-3'	5'-AGATGCCAGACATGAGGTTGA-3'
<i>Dmc1</i>	5'-GGAGGTGGCATTGAAAGTATGG-3'	5'-GCGATCTGGACGAAAGTATTTT-3'
<i>Ccdc155</i>	5'-CGAGCTATCTGGACATCCTTTC-3'	5'-GGCCTTGAAGTCCGCTTCTC-3'
<i>Prdm9</i>	5'-AGATACAGGGAAATTCGAGTGGA-3'	5'-GGTAACACATGAAAGCTGGTCT-3'
<i>Msh5</i>	5'-CCTGGGCATTGCTTACTATGAC-3'	5'-TGGCAGAAGTATGATTTCCAGTC-3'
<i>Phlda2</i>	5'-CTCCGACGAGATCCTTTGCG-3'	5'-ACACGTACTTAGAGGTGTGCTC-3'
<i>Foxf1</i>	5'-ACGCCGTTTACTCCAGCTC-3'	5'-CGTTGTGACTGTTTTGGTGAAG-3'
<i>Nkx1-1</i>	5'-CCCCTGTGGACGATACTGC-3'	5'-CTCGCACACCGACAGGTAG-3'
<i>Rhox10</i>	5'-GCAAGAAGTACACCAATGCC-3'	5'-GTTGTTTCGAGGTTCCAGATGTAG-3'
<i>Nanos3</i>	5'-ATGGGGACTTTCAATCTTTGGAC-3'	5'-GTTTGCAGAATGAACATAAGCGT-3'
<i>Inca1</i>	5'-ATGCCTCAGCCGTATGGAGAT-3'	5'-GCCCTCAGAATGGTGAATGTA-3'
<i>Pou5f1</i>	5'-GGCTTCAGACTTCGCCTCC-3'	5'-AACCTGAGGTCCACAGTATGC-3'
<i>Upp1</i>	5'-ACCGCTACGCCATGTATAAG-3'	5'-AAACTCCGGCTTGAAGCACTC-3'
<i>Utf1</i>	5'-ACCCTTCGATAACCAGATCCG-3'	5'-CAGGTTTCGCTTTCCTCCGAG-3'
<i>Asb9</i>	5'-GTATGTGGCTTGTAAAAACCAGC-3'	5'-AGCGTTTTCGCTCCGAAATCCAT-3'
<i>Sohlh1</i>	5'-CGGGCCAATGAGGATTACAGA-3'	5'-TCTCGCTTCTCTCTCGCT-3'
<i>Clic6</i>	5'-CCCAGGATGAGGCGATTG-3'	5'-GTCCTTCAACTCGGGTTCT-3'
<i>Rrad</i>	5'-ATGACCGTTCTACTGTGGA-3'	5'-TGGACCCGGAGTCTGAGG-3'
<i>Mobp</i>	5'-GCATCTGCAAGAGCGGTTG-3'	5'-GGCATCAGAGGGGACTTTGG-3'
<i>Pxt1</i>	5'-ATGCAGCTTAGACACATTGGG-3'	5'-ACCAGCGCCACAAAAGGAG-3'

Stra8: stimulated by retinoic acid gene 8; *Mtl5*: metallothionein-like 5; *Egr4*: early growth response 4; *Dmc1*: DNA meiotic recombinase 1; *Ccdc155*: coiled-coil domain containing 155; *Prdm9*: PR domain containing 9; *Msh5*: mutS homolog 5; *Phlda2*: pleckstrin homology-like domain, family A, member 2; *Foxf1*: forkhead box F1; *Nkx1-1*: NK1 homeobox 1; *Rhox10*: reproductive homeobox 10; *Nanos3*: nanos C2HC-type zinc finger 3; *Inca1*: cyclin A1 interacting protein 1; *Pou5f1*: POU domain, class 5, transcription factor 1; *Upp1*: uridine phosphorylase 1; *Utf1*: undifferentiated embryonic cell transcription factor 1; *Asb9*: ankyrin repeat and SOCS box-containing 9; *Sohlh1*: spermatogenesis- and oogenesis-specific basic helix-loop-helix 1; *Clic6*: chloride intracellular channel 6; *Rrad*: ras-related associated with diabetes; *Mobp*: myelin-associated oligodendrocytic basic protein; *Pxt1*: peroxisomal, testis-specific 1

RESULTS

Morphological analysis of *Stra8*^{-/-} mouse testes during the first wave of spermatogenesis

The offspring of heterozygous mice were genotyped by PCR amplification of testicular DNA fragments. Fragments of 316 bp and 200 bp were amplified from DNA extracts from heterozygous testes, while fragments of 200 bp and 316 bp were detected from *Stra8*^{-/-} and WT testes, respectively (Figure 1a).

Spermatogenesis in *Stra8*^{-/-} mice is arrested in meiotic prophase I and the testes undergo morphological changes during the first wave of spermatogenesis. Therefore, testes of *Stra8*^{+/+} and *Stra8*^{-/-} mice were collected at 5–12 dpp and tissue sections were stained with HE and evaluated by optical microscopy to identify the earliest point at which morphological differences in germ cells could be detected. This information was also important for selecting RNA-Seq samples. At 5, 6, and 7 dpp, only spermatogonia and Sertoli cells were observed in WT testis (Figure 1b–1d, left). Some spermatogonia showed more intense staining of the cells that were located in the adluminal compartment of seminiferous tubules, which then migrated to the basal lamina of the tubules at 8 dpp and 9 dpp (Figure 1e and 1f, left). In addition, the prospermatogonia transitioned to type A and B spermatogonia. Subsequently, at 10 dpp and 11 dpp, the diameter of the seminiferous tubules increased and the number of type B spermatogonia increased (Figure 1g and 1h, left). Primary spermatocytes first appeared at 12 dpp (Figure 1i, left). All types of germ cells were contained in the adult mouse testis (Figure 1j, left). There were no obvious differences in testicular histomorphology between *Stra8*^{-/-} and WT mice from 5 to 11 dpp (Figure 1b–1i). However, at 12 dpp, there were significantly fewer primary spermatocytes in *Stra8*^{-/-} mouse testes than in WT testes, and vacuoles appeared ($P < 0.05$; Figure 1i).

In accordance with these observations, adult *Stra8*^{-/-} mice are infertile and lack meiotic and postmeiotic cells (Figure 1j).

Germ cell counts in developing testes

Germ cells were counted by immunofluorescence staining of the DEAD (Asp-Glu-Ala-Asp) box polypeptide 4 (Ddx4), which is a specific marker expressed in the cytoplasm of germ cells. The number and signal intensity of Ddx4-positive cells increased gradually in the developing testis (Figure 2). In accordance with the HE staining at 5–11 dpp, there was no significant difference in the number and signal intensity of Ddx4-positive cells between *Stra8*^{-/-} and *Stra8*^{+/+} testes (Figure 2a–2g and 2i). However, at 12 dpp, the number of Ddx4-positive cells decreased significantly in *Stra8*^{-/-} mice compared with that in the WT mice ($P < 0.05$, $n \geq 6$; Figure 2h and 2i). Therefore, testes were obtained from *Stra8*^{-/-} and *Stra8*^{+/+} mice at 11 dpp for further RNA-Seq analysis.

Identification of DEGs in *Stra8*^{-/-} testes

To investigate the DEGs associated with *Stra8* deficiency, we generated a RNA-Seq profile of the transcriptome of *Stra8*^{-/-} testes and identified 40 downregulated transcripts and 56 upregulated transcripts in *Stra8*^{-/-} testes compared with the WT ($P < 0.05$).

GO analysis of the distribution of gene functions revealed that the DEGs were predominantly involved in biological processes, cellular components, and molecular functions including reproduction, reproductive process, and transcription (Figure 3). Genes often interact with each other in biological functions; therefore, we performed pathway enrichment analysis of 58 RNAs encoded by the DEGs. The top 20 KEGG enrichment and term types are shown in Figure 4. These DEGs were enriched in the pathways of spliceosome, RNA transport and Toll-like receptor signaling. They also involved in the KEGG pathway terms cellular processes, environmental information processing, genetic information processing, human disease and organismal systems.



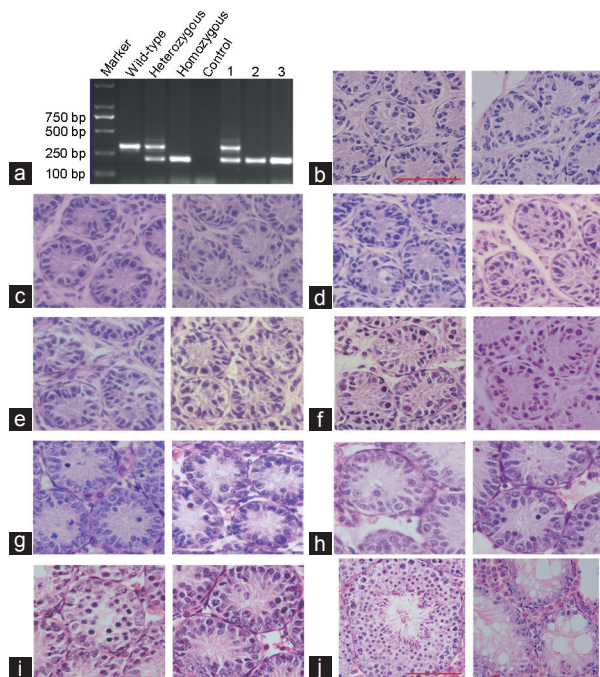


Figure 1: Histological analysis of testis from pubescent *Stra8*^{-/-} mice. (a) Genotyping of *Stra8*^{-/-} mice. Marker: DM2000 Plus II DNA Marker. (b–j) Hematoxylin and eosin staining of testes sections from WT and *Stra8*^{-/-} mice. (b–i) Left, sections from WT testes at 5–12 dpp; right, sections from homozygous testes at 5–12 dpp. (j) Left, testis sections from WT adult mice; right, testis sections from homozygous adult mice ($n \geq 6$; scale bars = 50 μm). WT: wild-type mouse; Heterozygous type: *Stra8*^{+/-} mouse; homozygous type: *Stra8*^{-/-} mouse; Control: water; 1–3: genotyping of three *Stra8* knockout mice. *Stra8*: stimulated by retinoic acid gene 8.

Role of DEGs in *Stra8*-mediated regulation of spermatogenesis

From the FPKM value and previous reports, we identified 21 DEGs directly or indirectly related to spermatogenesis. In addition to *Stra8*, the results of qRT-PCR analysis of the expression levels of the 21 DEGs were consistent with the results of RNA-Seq analysis. Testis expressions of metallothionein-like 5 (*Mt15*), DNA meiotic recombinase 1 (*Dmc1*), coiled-coil domain containing 155 (*Ccdc155*), inhibitor of CDK, cyclin A1 interacting protein 1 (*Inca1*), mutS homolog 5 (*Msh5*), and PR domain containing 9 (*Prdm9*) were downregulated, while reproductive homeobox10 (*Rhox10*), early growth response 4 (*Egr4*), uridine phosphorylase 1 (*Upp1*), undifferentiated embryonic cell transcription factor 1 (*Utf1*), POU domain, class 5, transcription factor 1 (*Pou5f1*), nanos C2HC-type zinc finger 3 (*Nanos3*), ankyrin repeat and SOCS box-containing 9 (*Asb9*), spermatogenesis- and oogenesis-specific basic helix-loop-helix1 (*Sohlh1*), peroxisomal, testis-specific 1 (*Pxt1*), pleckstrin homology-like domain, family A, member 2 (*Phlda2*), forkhead box F1 (*Foxf1*), NK1 homeobox1 (*Nkx1-1*), ras-related associated with diabetes (*Rrad*), chloride intracellular channel 6 (*Clic6*), and myelin-associated oligodendrocytic basic protein (*Mobp*) were upregulated (Figure 5a).

Of the 21 DEGs, we analyzed the expression levels of seven corresponding proteins by western blot (Figure 5b). In accordance with the levels of DEG expression determined by RNA-Seq and qRT-PCR analyses, the protein levels of *Rhox10*, *Nanos3*, *Egr4*, and *Asb9* were significantly increased in *Stra8*^{-/-} testes compared with those in WT testes ($P < 0.05$). By contrast, there were no significant differences in the protein levels of *Pou5f1*, *Msh5*, and *Dmc1* between WT and KO testes. We further detected the cellular distribution of *Nanos3*, *Egr4*,

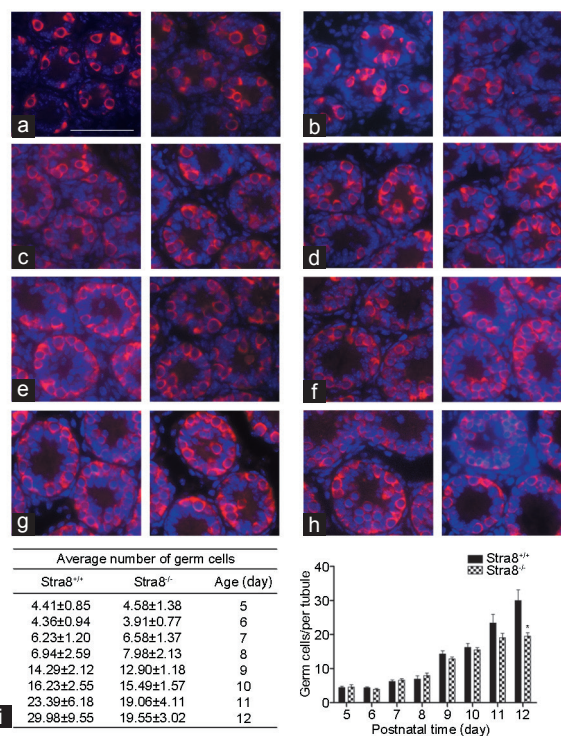


Figure 2: Germ cell counts in developing testes. (a–h) Immunofluorescence staining for Ddx4 (a specific germ cell marker) at 5–12 dpp. Left, sections from wild-type testes at 5–12 dpp; right, sections from *Stra8* homozygous testes at 5–12 dpp. Immunolabelling of Ddx4 (red), and DAPI (blue). $n \geq 6$; scale bars = 50 μm . (i) Average number of Ddx4-positive spermatogenic cells per tubule in cross-section ($n \geq 6$, mean \pm standard deviation, $^*P < 0.05$). *Stra8*: stimulated by retinoic acid gene 8; DAPI: diamidino-phenyl-indole.

Asb9, and *Msh5* in WT and KO testes by immunohistochemistry or immunofluorescence analysis (Figure 5c). *Nanos3* protein was located in the cytoplasm of spermatogonia, which showed an obvious increase in KO testes compared with WT testes. *Egr4* was weakly expressed in spermatogonia and early spermatocytes of wild-type mouse testes, but showed higher intensity in homozygous spermatocytes. *Asb9* had a similar pattern and tend of expression to *Egr4*, but the expression of *Msh5* was obviously reduced in homozygous testes, and it mainly appeared in the nucleus of spermatocytes. *Utf1*, as an undifferentiated marker, was expressed in the basal spermatogonia and the expression intensity was enhanced in KO testes.

Regulatory network involving *Stra8* in spermatogenesis

Different proteins often form complexes through complicated interactions to perform their biological functions. A literature review and protein–protein interaction network analysis of the 21 DEGs indicated that *Stra8* plays a variety of roles in multiple stages of spermatogenesis through cooperative interactions with the genes listed. We established a preliminary regulatory network of *Stra8* during spermatogenesis (Figure 6). In addition to the roles in spermatogonial differentiation and meiotic prophase I, *Stra8* is implicated in the establishment of SSCs, spermatogonial proliferation, self-renewal, and physiological processes.

DISCUSSION

Spermatogenesis is a multifaceted process by which SSCs undergo mitotic and meiotic divisions, eventually giving rise to haploid spermatozoa. *Stra8* plays a critical role in mammalian spermatogenesis, and mutations

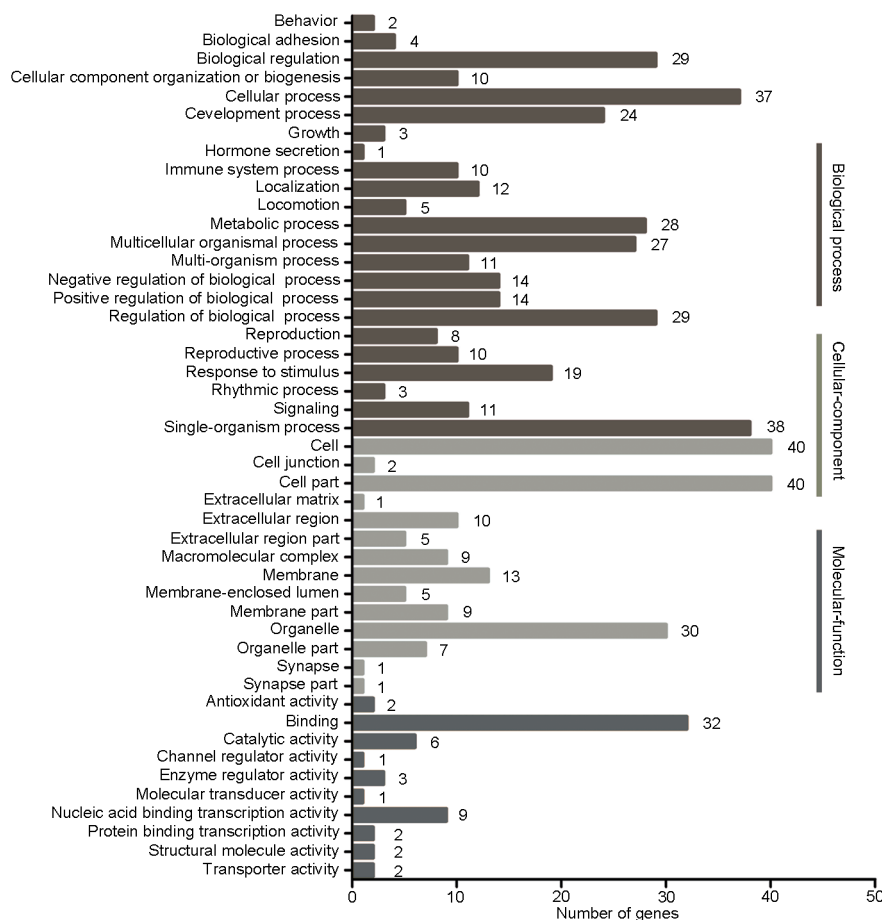


Figure 3: Gene ontology functional classification of differentially expressed genes. All gene ontology terms are grouped into three ontologies: biological process, cellular component, and molecular function.

are associated with increased risk of azoospermia and oligozoospermia in the Han Chinese population.¹ This phenomenon has been demonstrated in previous studies; however, the mechanism underlying the function of *Stra8* in spermatogenesis is still not fully understood.

In this study, we investigated the function of *Stra8* and its potential regulatory networks during spermatogenesis using male *Stra8* KO mice. The choice of 5–12 dpp testes was dictated by the expression of *Stra8*, which started at 5 dpp, reached a peak at 10 dpp, and then began to decline⁴ and was, therefore, suitable for investigating the mechanism underlying the functions of *Stra8*. There were no apparent differences in the morphology and number of germ cells in WT and *Stra8*^{-/-} testes at 11 dpp. The DEGs identified at 11 dpp were most likely due to *Stra8* deficiency. According to the FPKM value and previous reports, we demonstrated that 21 of these DEGs were directly or indirectly associated with spermatogenesis. Thus, it can be speculated that *Stra8* regulates spermatogenesis by coordinating with these genes.

The role of Stra8 in establishment of SSCs, cell proliferation, self-renewal, and maintenance of the undifferentiated state of spermatogonia

In mammals, primordial germ cells (PGCs) and prospermatogonia (ProSG) transform into SSCs under certain microenvironmental conditions.¹⁰ SSCs maintain long-term male fertility via a highly controlled process of self-renewal and maintenance of the undifferentiated state. Spermatogonial self-renewal is ensured by three elements: maintained

survival, stable proliferation, and a continuous state of undifferentiation. These three elements are not isolated but are completely interdependent.

Testes of adult *Stra8* KO mice are much smaller than those of age-matched WT mice, lacking meiotic and postmeiotic cells.^{11,12} However, aged testes from *Stra8* KO mice progressively enlarged compared with WT testis, in which seminiferous tubules were filled with type A spermatogonia which even spilled into the interstitium due to the presence of only a few tubule structures. The absence of *Stra8* gave rise to the accumulation of type A spermatogonia.¹ Saba *et al.*⁶ showed that *Stra8* was activated in testes containing the *Cyp26b1* mutation and germ cells entered meiosis prematurely. *Cyp26b1* and *Stra8* double KO testes display a disruption of meiosis but increased mitotic activity. These findings suggest that *Stra8* plays a role in spermatogonial proliferation and differentiation.

Rhox10 promotes the initial establishment of SSCs by suppressing the conversion of ProSG into differentiating A spermatogonia.¹³ *Stra8* is expressed in both undifferentiated and differentiated spermatogonia. The expression of *Rhox10* is translocated from the cytoplasm to the nucleus, which is similar to the pattern of *Stra8* expression. In this study, we noted a marked upregulation of *Rhox10* expression in *Stra8* KO testes, which indicated the involvement of *Stra8* in the establishment of SSCs by coordinating with *Rhox10*.

We also found obvious upregulation of the expression of *Utf1*, *Pou5f1*, and *Upp1* in *Stra8*^{-/-} testes, while *Inca1* expression was downregulated. *Utf1* plays a role in the prevention of embryonic stem (ES) cell differentiation. *Pou5f1* plays an essential role in the maintenance of the

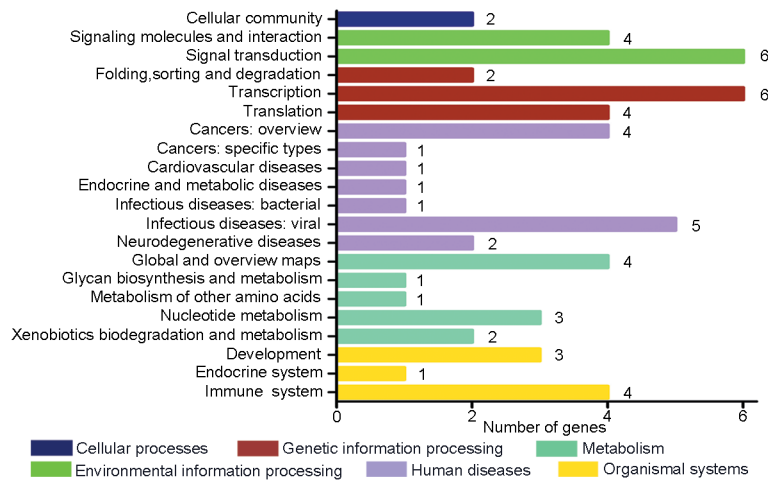


Figure 4: Pathway enrichment analysis of differentially expressed genes. Kyoto encyclopedia of genes and genomes classification of differentially expressed genes.

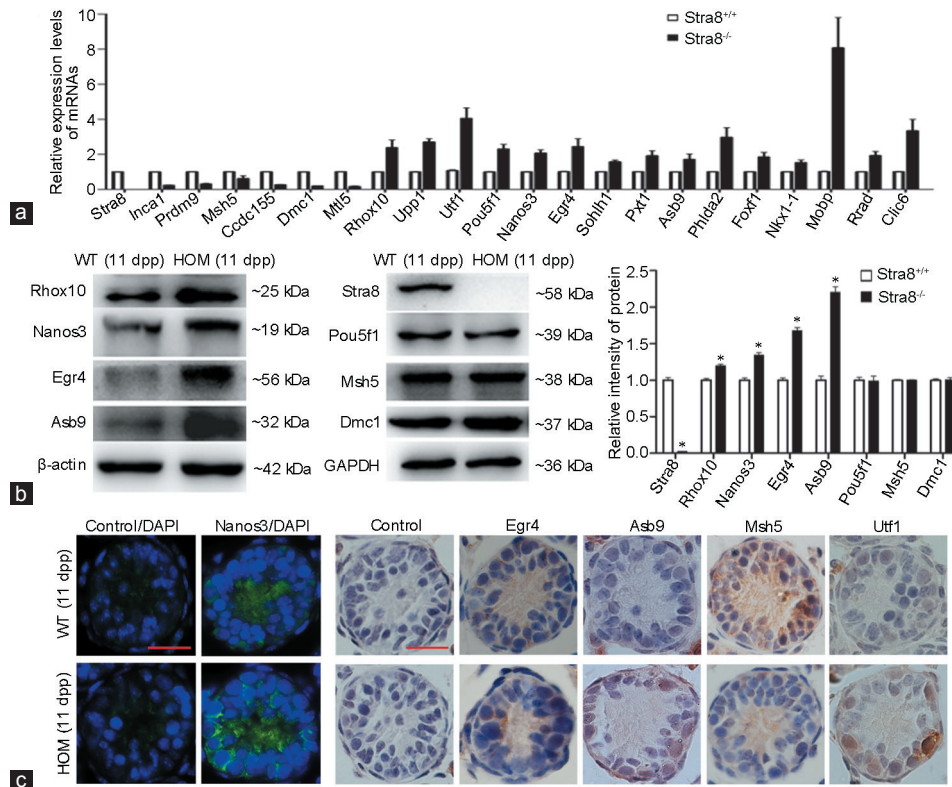


Figure 5: (a) Quantitative RT-PCR analysis of the DEGs involved in spermatogenesis. Data represent mean \pm s.d., and values were normalized to WT mRNA levels. All 21 DEGs were statistically significant ($P < 0.05$). (b) Western blot analysis of proteins extracted from *Stra8*^{-/-} testes at 11 dpp. Blots were probed with primary antibodies for the detection of *Stra8*, *Rhox10*, *Nanos3*, *Egr4*, *Asb9*, *Pou5f1*, *Msh5* and *Dmc1*. The protein levels of *Rhox10*, *Nanos3*, *Egr4*, and *Asb9* were significantly increased in HOM testes compared with WT testes ($*P < 0.05$). *Pou5f1*, *Msh5*, and *Dmc1* protein levels were not significantly different between WT and *Stra8* knockout testes. (c) Immunohistochemistry/immunofluorescence analysis of *Nanos3*, *Egr4*, *Asb9*, *Msh5*, and *Utf1* expression in WT and *Stra8* knockout testes; *Nanos3* (green), DAPI (blue). Scale bars = 10 μ m. RT-PCR: reverse transcription polymerase chain reaction; DAPI: diamidino-phenyl-indole; s.d.: standard deviation; WT: wild-type; HOM: homozygous; dpp: days postpartum; DEGs: differentially expressed genes. *Stra8*: stimulated by retinoic acid gene 8; *Mt15*: metallothionein-like 5; *Egr4*: early growth response 4; *Dmc1*: DNA meiotic recombinase 1; *Ccdc155*: coiled-coil domain containing 155; *Prdm9*: PR domain containing 9; *Msh5*: mutS homolog 5; *Phlda2*: pleckstrin homology-like domain, family A, member 2; *Foxf1*: forkhead box F1; *Nkx1-1*: NK1 homeobox 1; *Rhox10*: reproductive homeobox 10; *Nanos3*: nanos C2HC-type zinc finger 3; *Inca1*: cyclin A1 interacting protein 1; *Pou5f1*: POU domain, class 5, transcription factor 1; *Upp1*: uridine phosphorylase 1; *Utf1*: undifferentiated embryonic cell transcription factor 1; *Asb9*: ankyrin repeat and SOCS box-containing 9; *Sohlh1*: spermatogenesis- and oogenesis-specific basic helix-loop-helix 1; *Clic6*: chloride intracellular channel 6; *Rrad*: ras-related associated with diabetes; *Mobb*: myelin-associated oligodendrocytic basic protein; *Pxt1*: peroxisomal, testis-specific 1.

stem cell state and induces rapid proliferation of ES cells through binding to the regulatory region of *Utf1* via a variant octamer sequence together

with Sox-2 leading to activation of *Utf1*.¹⁴⁻¹⁷ *Inca1* is involved in regulating cell cycle, detecting and repairing gene damage, and preventing abnormal

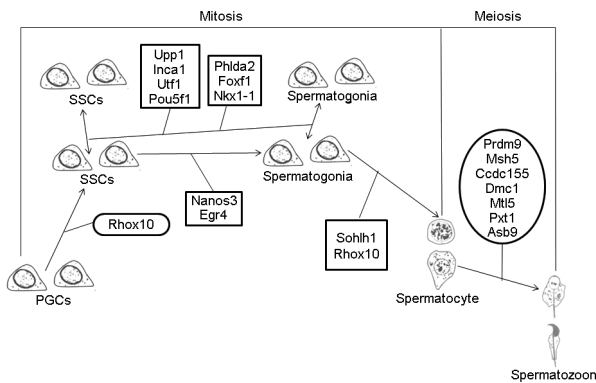


Figure 6: Regulatory network involving *Stra8* in spermatogenesis. SSC: spermatogonial stem cell; PGC: primordial germ cell. *Stra8*: stimulated by retinoic acid gene 8; *Mtl5*: metallothionein-like 5; *Egr4*: early growth response 4; *Dmc1*: DNA meiotic recombinase 1; *Ccdc155*: coiled-coil domain containing 155; *Prdm9*: PR domain containing 9; *Msh5*: mutS homolog 5; *Phlda2*: pleckstrin homology-like domain, family A, member 2; *Foxf1*: forkhead box F1; *Nkx1-1*: NK1 homeobox 1; *Rhox10*: reproductive homeobox 10; *Nanos3*: nanos C2HC-type zinc finger 3; *Inca1*: cyclin A1 interacting protein 1; *Pou5f1*: POU domain, class 5, transcription factor 1; *Upp1*: uridine phosphorylase 1; *Utf1*: undifferentiated embryonic cell transcription factor 1; *Asb9*: ankyrin repeat and SOCS box-containing 9; *Sohlh1*: spermatogenesis- and oogenesis-specific basic helix-loop-helix 1; *Pxt1*: peroxisomal, testis-specific 1.

proliferation.^{18,19} Targeted mutation of *Upp1* causes disruption of cell proliferation, uracil DNA damage, and p53 activation.²⁰ *Utf1*, *Pou5f1*, *Inca1* and *Upp1* are all associated with cell cycle progression and cell proliferation. It can be speculated that *Stra8* cooperates with these genes in stable proliferation and self-renewal of spermatogonia.

In male mice, *Nanos3* is fully downregulated before differentiation of type B spermatogonia and plays important roles in both the survival and maintenance of undifferentiated spermatogonia.^{21,22} Moreover, *Egr4* was highly expressed in SSCs, and decreased rapidly during differentiation, which indicated the involvement of *Egr4* in maintaining the SSC population.²³ With the first appearance of *Stra8* expression in the late undifferentiated spermatogonia,¹ the expression of *Nanos3* and *Egr4* increased significantly in *Stra8*^{-/-} testes. It can be speculated that this pattern of expression has an effect on the maintenance of undifferentiated SSCs. Furthermore, it is likely that *Stra8* performs functions in the maintenance of the undifferentiated state through the regulation of *Nanos3* and *Egr4*, although the precise details of the regulatory network remain to be established.

The role of *Stra8* in the differentiating spermatogonia

When spermatogonia begin to differentiate, the activity of pluripotent genes is downregulated and the self-renewal ability is lost. Once differentiation is initiated, it is irreversible. The expression level of *Sohlh1* was significantly increased in *Stra8* KO testes. *Sohlh1* is critical for spermatogonial differentiation and is expressed mainly in differentiating spermatogonia. *Sohlh1* and *Sohlh2* function cooperatively and directly to repress *Stra8* expression by binding to E-Boxes in its promoter.^{8,24} *Rhox10* is detected during the whole process of spermatogonial differentiation.^{13,25} *Stra8*-deficient testes contain a significantly reduced proportion of type B spermatogonia.^{1,3,4} *Stra8* may promote differentiation of spermatogonia through regulation of *Sohlh1*, *Rhox10*, and other molecules to ensure *Stra8* downregulation during the mid-end stages of meiotic prophase I.

The role of *Stra8* in meiotic prophase I

In mammalian spermatogenesis, meiosis is a specialized cellular process. *Stra8*, a marker of meiosis initiation, is required for germ cells to undergo meiotic prophase. *Stra8*^{-/-} testes exhibit heterosynapsis or extensive asynapsis.¹¹ In addition, *Stra8* is reported to be a potential component of an unidentified cell cycle surveillance system, such as a checkpoint, in response to errors in chromosome synapsis or recombination.¹² Many studies have demonstrated the critical role of *Stra8* in meiosis; however, the underlying mechanism of spermatogonial differentiation and meiotic initiation remains to be elucidated. In the current study, we found that the expression levels of some meiosis-related genes changed significantly during spermatogenesis, which may provide a theoretical basis for further investigations of the functions of *Stra8*.

Stra8-deficiency results in arrest of spermatogenesis in leptotene prophase and failure of the transition to the zygotene/pachytene stages. The expression levels of *Prdm9* and *Msh5* were significantly reduced in *Stra8* KO testes. *Prdm9*, which plays a key role in the initiation of meiotic events, was highly expressed in preleptonema and early leptotema. Male *Prdm9*-deficient mice are infertile, with meiosis arrested before the mid-pachytene stage.^{26,27} *Msh5* is highly expressed at the early preleptotene to zygotene stages, with lower expression at the pachytene stage. In *Msh5* mutant mice, meiosis is arrested around the zygotene stage, with a high level of asynapsis and persistent unrepaired DNA double-strand breaks.^{28,29} The *Stra8* expression pattern is consistent with that of *Prdm9* and *Msh5* in spermatocytes. We postulate that *Stra8* directly or indirectly targets the regulation of *Prdm9* and *Msh5* to ensure the successful progress of meiosis prophase I.

We also identified significant changes in the expression of some other meiosis-associated genes. Both *Egr4*^{23,30} and *Mtl5* (*tesmin*)³¹ are cytoplasmic and nuclear shuttle proteins that predominantly function in the early stage of pachytene spermatocytes. Genecards software analysis shows that *Egr4* binds to the promoter of the *CCDC155* gene. *Ccdc155* (*Kash5*) is localized predominantly at the telomere from the leptotene to diplotene stages in spermatocytes. *Kash5* combines with *SUN1* to form the *SUN-Kash* nuclear envelope bridge, which mediates the meiotic homolog pairing.³² *Dmc1* is essential for the correct execution of meiotic recombination, and spermatogenesis in *Dmc1*-mutated testes progresses only to the late leptotene and early pachytene.^{33,34} *Pxt1* interacts with the apoptosis regulator *BAT3*, and *c-myc-Pxt1* transgenic mouse testes revealed arrest of spermatogenesis in pachytene spermatocytes.³⁵ *Asb9*, a specific marker of active spermatogenesis, is strongly expressed in pachytene spermatocytes and round spermatids. However, its function in spermatocytes has not yet been reported.³⁶

In *Stra8* KO testes, the expression of *Egr4*, *Pxt1*, and *Asb9* was significantly upregulated, while *Ccdc155*, *Dmc1*, and *Mtl5* expression was downregulated. Interestingly, *Stra8* is not present in pachytene spermatocytes and there is no evidence that *Stra8* directly regulates these genes. We hypothesize that a defect in meiosis I indirectly results in changes in the expression of these genes. A recent study³⁷ offered another possible explanation for this change based on the known ability of RA to regulate spermatogonial differentiation and meiotic initiation. Endo *et al.*³⁷ demonstrated that RA also regulates the initiation of spermatid elongation and release of spermatozoa. The indirect regulation of pachytene spermatocyte-related genes by *Stra8* may be due, in part, to RA produced by pachytene spermatocytes.

The role of *Stra8* in physiological processes

Phlda2 is negatively correlated with cell migration and invasion and inhibits glycogen accumulation.³⁸ *Foxf1* promotes angiogenesis and

regulates embryonic and pluripotent stem cell differentiation.³⁹ Energy homeostasis is regulated mainly by factors produced in the hypothalamus and the brainstem. Nkx1-1 (homeobox gene *Sax2*), which is a key regulator of organ development, maintains the steady state of energy homeostasis.⁴⁰

Studies to date have focused on the functions of *Phlda2*, *Foxf1*, and *Nkx1-1* in embryonic development, angiogenesis, and energy homeostasis. Currently, there is no evidence of a direct link between *Phlda2*, *Foxf1*, *Nkx1-1*, and survival or self-renewal of spermatogonia. However, expression of these genes at the mRNA level increased in *Stra8*^{-/-} mice, leading us to postulate a role in attachment of spermatogonia to the seminiferous tubule membrane, provision of energy for cell proliferation in mitosis, and maintenance of spermatogonia survival, with a possible indirect role in spermatogenesis.

Moreover, although *Mobb*,⁴¹ *Rrad*,⁴² and *Clic6*^{43,44} were not directly related to spermatogenesis, their expression was directly related to *Stra8*, with an obvious increase in *Stra8*-deficient testes. Spermatogenesis is a complex and highly precise physiological processes, which may involve many unknown mechanisms that require these molecules although this remains to be established.

CONCLUSION

In this study, we identified 21 DEGs related to spermatogenesis that possibly coordinate with *Stra8* in this process. Combined with analysis of relevant reports, we provide evidence indicating that *Stra8* is a multifunctional protein involved in spermatogenesis. In addition to the major function in spermatogonial differentiation, *Stra8* is also implicated in meiotic initiation, the establishment and maintenance of SSCs, cell proliferation, self-renewal, undifferentiation, and other physiological processes. The identification of *Stra8*-related genes and establishment of its regulatory network provides an improved understanding of the role of *Stra8* in spermatogenesis, as well as a theoretical basis for its involvement in mammalian reproduction and the implications of dysregulation on germline tumors and infertility.

AUTHOR CONTRIBUTIONS

HTM designed and carried out experiments; CMN wrote article and performed the experiments; JX, YYS, and MMX collected literatures and analyzed data; YQH participated in the design of the study; and YZ designed the study. All authors read and approved the final version of the manuscript.

COMPETING INTERESTS

All authors declared no competing interests.

ACKNOWLEDGMENTS

This work was supported by the National Natural Science Foundation of China (Number 31371174), the Natural Science Foundation of Jiangsu Province, China (Number BK20131230), and the Postgraduate Research and Practice Innovation Program of Jiangsu Province, China (KYCX17-1893). We thank Dr. Wilkinson (University of California, USA) for kindly providing *Rhox10* antibody.

REFERENCES

- Endo T, Romer KA, Anderson EL, Baltus AE, de Rooij DG, *et al*. Periodic retinoic acid-STRA8 signaling intersects with periodic germ-cell competencies to regulate spermatogenesis. *Proc Natl Acad Sci U S A* 2015; 112: 2347–56.
- Zhou Q, Nie R, Li Y, Friel P, Mitchell D, *et al*. Expression of stimulated by retinoic acid gene 8 (*Stra8*) in spermatogenic cells induced by retinoic acid: an *in vivo* study in Vitamin A-sufficient postnatal murine testes. *Biol Reprod* 2008; 79: 35–42.
- Oulad-Abdelghani M, Bouillet P, Décimo D, Gansmuller A, Heyberger S, *et al*. Characterization of a premeiotic germ cell-specific cytoplasmic protein encoded by *Stra8*, a novel retinoic acid-responsive gene. *J Cell Biol* 1996; 135: 469–77.
- Feng CW, Bowles J, Koopman P. Control of mammalian germ cell entry into meiosis. *Mol Cell Endocrinol* 2014; 382: 488–97.
- Potter SJ, DeFalco T. Role of the testis interstitial compartment in spermatogonial stem cell function. *Reproduction* 2017; 153: 151–62.
- Saba R, Wu Q, Saga Y. CYP26B1 promotes male germ cell differentiation by suppressing STRA8-dependent meiotic and STRA8-independent mitotic pathways. *Dev Biol* 2014; 389: 173–81.
- Chen W, Jia W, Wang K, Si X, Zhu S, *et al*. Distinct roles for CBP and p300 on the RA-mediated expression of the meiosis commitment gene *Stra8* in mouse embryonic stem cells. *PLoS One* 2013; 8: e66076.
- Desimio MG, Campolo F, Dolci S, De Felici M, Farini D. SOHLH1 and SOHLH2 directly down-regulate STIMULATED BY RETINOIC ACID 8 (*STRA8*) expression. *Cell Cycle* 2015; 14: 1036–45.
- Zhang T, Murphy MW, Gearhart MD, Bardwell VJ, Zarkower D. The mammalian doublesex homolog *DMRT6* coordinates the transition between mitotic and meiotic developmental programs during spermatogenesis. *Development* 2014; 141: 3662–71.
- McCarrey JR. Toward a more precise and informative nomenclature describing fetal and neonatal male germ cells in rodents. *Biol Reprod* 2013; 89: 47.
- Anderson EL, Baltus AE, Roepers-Gajadien HL, Hassold TJ, de Rooij DG. *Stra8* and its inducer, retinoic acid, regulate meiotic initiation in both spermatogenesis and oogenesis in mice. *Proc Natl Acad Sci U S A* 2008; 105: 14976–80.
- Baltus AE, Menke DB, Hu YC, Goodheart ML, Carpenter AE, *et al*. In germ cells of mouse embryonic ovaries, the decision to enter meiosis precedes premeiotic DNA replication. *Nat Genet* 2006; 38: 1430–4.
- Song HW, Bettogowda A, Lake BB, Zhao AH, Skarbræk D, *et al*. The homeobox transcription factor *RHOX10* drives mouse spermatogonial stem cell establishment. *Cell Rep* 2016; 17: 149–64.
- Kooistra SM, van den Boom V, Thummer RP, Johannes F, Wardenaar R, *et al*. Undifferentiated embryonic cell transcription factor 1 regulates ESC chromatin organization and gene expression. *Stem Cells* 2010; 28: 1703–14.
- Lin CH, Yang CH, Chen YR. *UTF1* deficiency promotes retinoic acid-induced neuronal differentiation in P19 embryonal carcinoma cells. *Int J Biochem Cell Biol* 2012; 44: 350–7.
- Niwa H, Masui S, Chambers I, Smith AG, Miyazaki J. Phenotypic complementation establishes requirements for specific POU domain and generic transactivation function of Oct-3/4 in embryonic stem cells. *Mol Cell Biol* 2002; 22: 1526–36.
- Nishimoto M, Miyagi S, Yamagishi T, Sakaguchi T, Niwa H, *et al*. Oct-3/4 maintains the proliferative embryonic stem cell state via specific binding to a variant octamer sequence in the regulatory region of the *UTF1* locus. *Mol Cell Biol* 2005; 25: 5084–94.
- Bäumer N, Tickenbrock L, Tschanter P, Lohmeyer L, Diederichs S, *et al*. Inhibitor of cyclin-dependent kinase (CDK) interacting with cyclin A1 (*INCA1*) regulates proliferation and is repressed by oncogenic signaling. *J Biol Chem* 2011; 286: 28210–22.
- Li XB, Chen J, Deng MJ, Wang F, Du ZW, *et al*. Zinc finger protein *HZF1* promotes K562 cell proliferation by interacting with and inhibiting *INCA1*. *Mol Med Rep* 2011; 4: 1131–7.
- Cao Z, Ma J, Chen X, Zhou B, Cai C, *et al*. Uridine homeostatic disorder leads to DNA damage and tumorigenesis. *Cancer Lett* 2016; 372: 219–25.
- Suzuki H, Sada A, Yoshida S, Saga Y. The heterogeneity of spermatogonia is revealed by their topology and expression of marker proteins including the germ cell-specific proteins *Nanos2* and *Nanos3*. *Dev Biol* 2009; 336: 222–31.
- Suzuki H, Tsuda M, Kiso M, Saga Y. *Nanos3* maintains the germ cell lineage in the mouse by suppressing both Bax-dependent and -independent apoptotic pathways. *Dev Biol* 2008; 318: 133–42.
- Hogarth CA, Mitchell D, Small C, Griswold M. *EGR4* displays both a cell- and intracellular-specific localization pattern in the developing murine testis. *Dev Dyn* 2010; 239: 3106–14.
- Toyoda S, Yoshimura T, Mizuta J, Miyazaki J. Auto-regulation of the *Sohlh1* gene by the *SOHLH2/SOHLH1/SP1* complex: implications for early spermatogenesis and oogenesis. *PLoS One* 2014; 9: e101681.
- Song HW, Dann CT, McCarrey JR, Meistrich ML, Cornwall GA. Dynamic expression pattern and subcellular localization of the *Rhox10* homeobox transcription factor during early germ cell development. *Reproduction* 2012; 143: 611–24.
- Sun F, Fujiwara Y, Reinholdt LG, Hu J, Saxl RL, *et al*. Nuclear localization of *PRDM9* and its role in meiotic chromatin modifications and homologous synapsis. *Chromosoma* 2015; 124: 397–415.
- Parvanov ED, Tian H, Billings T, Saxl RL, Spruce C, *et al*. *PRDM9* interactions with other proteins provide a link between recombination hotspots and the chromosomal axis in meiosis. *Mol Biol Cell* 2017; 28: 488–99.
- Lu X, Liu X, An L, Zhang W, Sun J, *et al*. The arabidopsis *MutS* homolog *AtMSH5* is required for normal meiosis. *Cell Res* 2008; 18: 589–99.
- Mahadevaiah SK, Bourc'his D, de Rooij DG, Bestor TH, Turner JM, *et al*. Extensive meiotic asynapsis in mice antagonises meiotic silencing of unsynapsed chromatin and consequently disrupts meiotic sex chromosome inactivation. *J Cell Biol* 2008; 182: 263–76.
- Tourtellotte WG, Nagarajan R, Auyeung A, Mueller C, Milbrandt J. Infertility associated with incomplete spermatogonial arrest and oligozoospermia in *Egr4*-deficient mice. *Development* 1999; 126: 5061–71.
- Olesen C, Møller M, Byskov AG. *Tesmin* transcription is regulated differently during male and female meiosis. *Mol Reprod Dev* 2004; 67: 116–26.



- 32 Morimoto A, Shibuya H, Zhu X, Kim J, Ishiguro K, *et al*. A conserved KASH domain protein associates with telomeres, SUN1, and dynactin during mammalian meiosis. *J Cell Biol* 2012; 198: 165–72.
- 33 Borgogno MV, Monti MR, Zhao W, Sung P, Argaraña CE, *et al*. Tolerance of DNA mismatches in Dmc1 recombinase-mediated DNA strand exchange. *J Biol Chem* 2016; 291: 4928–38.
- 34 Cloud V, Chan YL, Grubb J, Budke B, Bishop DK. Rad51 is an accessory factor for Dmc1-mediated joint molecule formation during meiosis. *Science* 2012; 337: 1222–5.
- 35 Forand A, Bernardino-Sgherri J. A critical role of PUMA in maintenance of genomic integrity of murine spermatogonial stem cell precursors after genotoxic stress. *Cell Res* 2009; 19: 1018–30.
- 36 Lee MR, Kim SK, Kim JS, Rhim SY, Kim KS. Expression of murine Asb-9 during mouse spermatogenesis. *Mol Cells* 2008; 26: 621–4.
- 37 Endo T, Freinkman E, de Rooij DG, Page DC. Periodic production of retinoic acid by meiotic and somatic cells coordinates four transitions in mouse spermatogenesis. *Proc Natl Acad Sci U S A* 2017; 114: 10132–41.
- 38 Tunster SJ, Van De Pette M, John RM. Isolating the role of elevated Phlda2 in asymmetric late fetal growth restriction in mice. *Dis Model Mech* 2014; 7: 1185–91.
- 39 Kalinichenko VV, Gusarova GA, Shin B, Costa RH. The forkhead box F1 transcription factor is expressed in brain and head mesenchyme during mouse embryonic development. *Gene Expr Patterns* 2003; 3: 153–8.
- 40 Simon R, Lufkin T, Bergemann AD. Homeobox gene *Sax2* deficiency causes an imbalance in energy homeostasis. *Dev Dyn* 2007; 236: 2792–9.
- 41 Laursen KB, Wong PM, Gudas LJ. Epigenetic regulation by RAR α maintains ligand-independent transcriptional activity. *Nucleic Acids Res* 2012; 40: 102–15.
- 42 Manning JR, Yin G, Kaminski CN, Magyar J, Feng HZ, *et al*. Rad GTPase deletion increases L-type calcium channel current leading to increased cardiac contraction. *J Am Heart Assoc* 2013; 2: e000459.
- 43 Friedli M, Guipponi M, Bertrand S, Bertrand D, Neerman-Arbez M, *et al*. Identification of a novel member of the CLIC family, CLIC6, mapping to 21q22.12. *Gene* 2003; 320: 31–40.
- 44 Griffon N, Jeanneteau F, Prieur F, Diaz J, Sokoloff P. CLIC6, a member of the intracellular chloride channel family, interacts with dopamine D (2)-like receptors. *Brain Res Mol Brain Res* 2003; 117: 47–57.

This is an open access journal, and articles are distributed under the terms of the Creative Commons Attribution-NonCommercial-ShareAlike 4.0 License, which allows others to remix, tweak, and build upon the work non-commercially, as long as appropriate credit is given and the new creations are licensed under the identical terms.

©The Author(s)(2018)

